

3D Printing Science FOSH Policy

- How to determine FOSH value?
- ROI
- Case study: syringe pump
- Public spending on science and technology

Michigan Tech

Michigan Technological University
Open Sustainability Technology
Research Group



How Much is Your FOSH Design Worth?

1. Downloaded Substitution Valuation (w, w/out discount rate i)

Pearce, J.M. (2015) Quantifying the Value of Open Source Hardware Development. *Modern Economy*, 6, 1-11. doi: 10.4236/me.2015.61001.

The downloaded substitution valuation uses the number of times that a FOSH design is accessed on the Internet to quantify the value of the design. The downloaded valuation for substitution savings, is:

$$V_D(t) = (C_p - C_f) \times P \times N_D(t)$$

where C_p is the cost to purchase a traditionally manufactured product, C_f is the marginal cost to fabricate it digitally using a distributed technique, P is the percent of downloads resulting in a product, and $N_D(t)$ is the number of times the digital design has been downloaded at time t . P is subject to error

$$V_{DT} = \sum_{t=1}^T (C_p(t) - C_f(t)) \times P \times \left(\frac{[N_D(t)]}{(1+i)^t} \right)$$

Michigan Tech

Michigan Technological University
Open Sustainability Technology
Research Group



2. Avoided Reproduction Value

$$V_R = h \times w \quad (2a)$$

where h is the number of design hours needed to replicate the product and w is the hourly wage of the workers needed to produce the replication. This method of capturing value can also be extrapolated to all firms (and individuals that would hire firms or freelance designers to complete the design) to obtain the total value to society and is given by:

$$\tilde{V}_n(t) = \sum_{t=1}^T \left(\frac{(h \times w \times P \times N_D(t))}{(1+i)^t} \right) \quad (2b)$$

where i is the discount rate and it is assumed that there is no variation in wages or design time efficiency. Taking both of these variables into account provides:

$$V_n(t) = \sum_{n=1}^J h_n \times w_n \quad (2c)$$

where the variable time to complete the design and wages needed to do it are taken into account for J types of jobs. To account for the value for all of time (t) :

$$V_{RT} = \sum_{t=1}^T \left[\frac{V_n(t)}{(1+i)^t} \right] = \sum_{t=1}^T \left[\frac{\sum_{n=1}^J h_n \times w_n}{(1+i)^t} \right] \quad (2d)$$

3. Market Savings Valuation (only in Future for now)

$$V_M(t) = M(t) - (C_f(t) \times N_M(t)) \quad (3a)$$

The sum of the market over T years can be calculated and converted to a net present total market value (V_{MT}) by:

$$V_{MT} = \sum_{t=1}^T \frac{[M(t) - (C_f(t) \times N_M(t))]}{(1+i)^t} \quad (3b)$$

where $M(t)$ is the current market in year t in US dollars and $N_M(t)$ is the total number of products of a specific type that make up market M .

Michigan Tech

Michigan Technological University
Open Sustainability Technology
Research Group



Secondary Stream of Value

All three core methods can be extended, as there are additional second order effects in providing value to the commons. Additional value can be tallied for educational benefits (V_{ED}), health benefits that increase longevity and productivity (V_{MED}), those that enhance science and engineering development (V_{SCI}), and a catch all of others (V_{OTH}). Thus, Equation 1(b) from the downloaded substitution valuation is expanded to provide the total value for all time:

$$V'_{DT} = V_{DT} + \sum_{t=1}^T \frac{[V_{ED}(t) + V_{MED}(t) + V_{SCI}(t) + V_{OTH}(t)]}{(1+i)^t} \quad (4a)$$

Similarly, Equation 2(d) from the avoided reproduction valuation method 2 becomes:

$$V'_{RT} = V_{RT} + \sum_{t=1}^T \frac{[V_{ED}(t) + V_{MED}(t) + V_{SCI}(t) + V_{OTH}(t)]}{(1+i)^t} \quad (4b)$$

Finally, in the market savings valuation, the total market for a given product would likely expand because of the lower costs, superior customization or a combination of both. As the cost of the product has decreased by S , an extra value, V_{EC} , is derived from expanding the market. Thus, the total value of market savings and these additional benefits (market total plus or V'_{MT} is now given by:

$$V'_{MT} = V_{MT} + \sum_{t=1}^T \frac{[V_{EC}(t) + V_{ED}(t) + V_{MED}(t) + V_{SCI}(t) + V_{OTH}(t)]}{(1+i)^t} \quad (4c)$$

Return on Investment (ROI)

Investment in scientific open source hardware can thus create a ROI that can be calculated by:

$$ROI = \frac{V_D(t) - I}{I} \quad (2)$$

Where I is the cost of the investment in the development of the FOSH scientific tool.

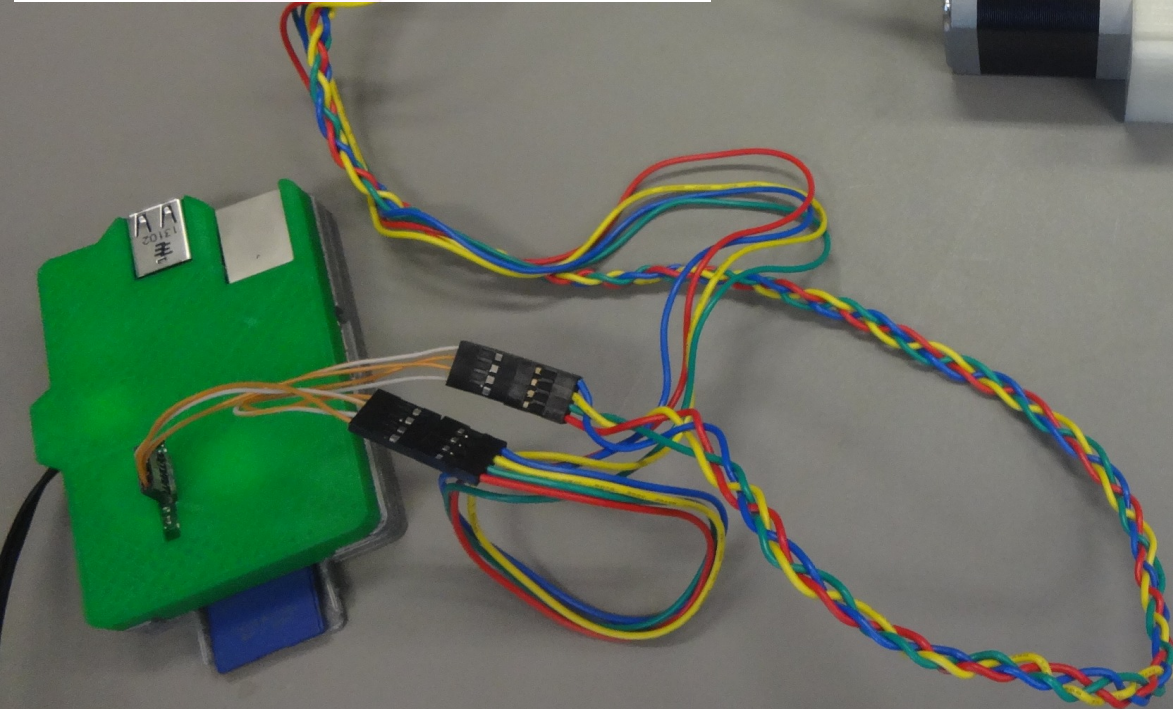
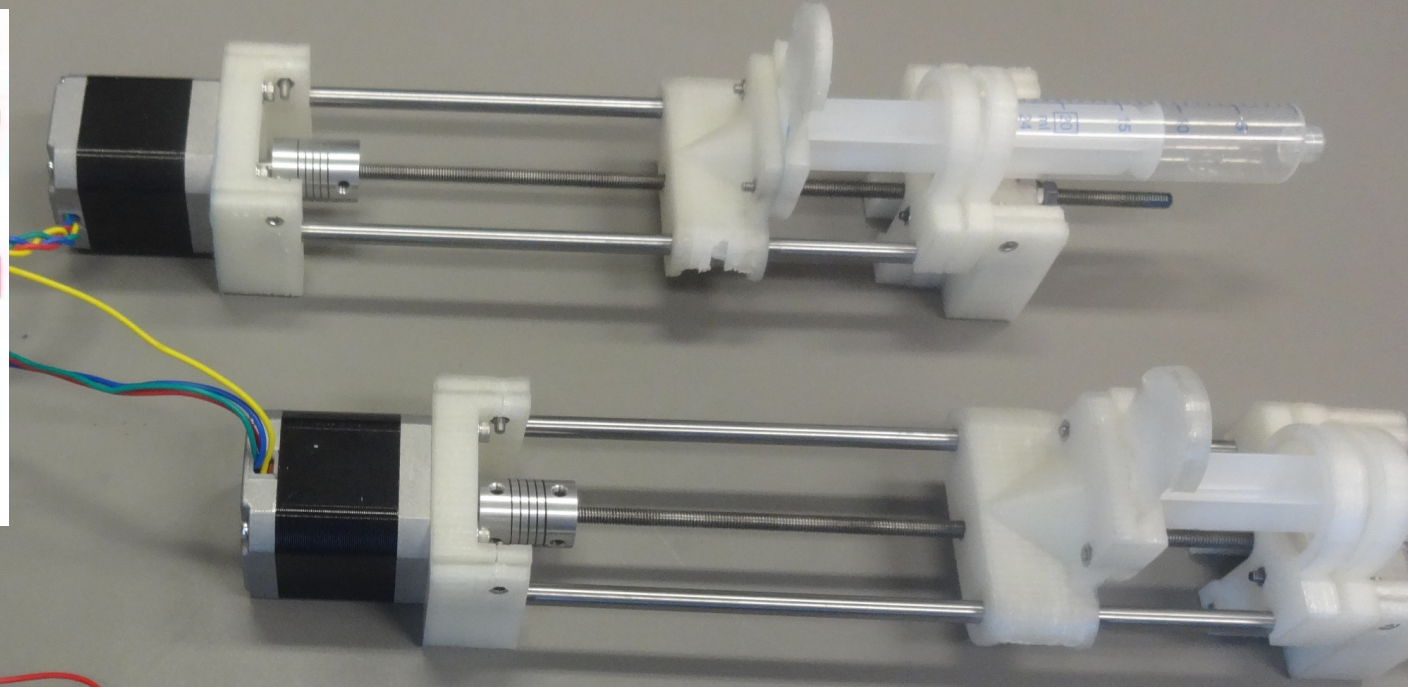
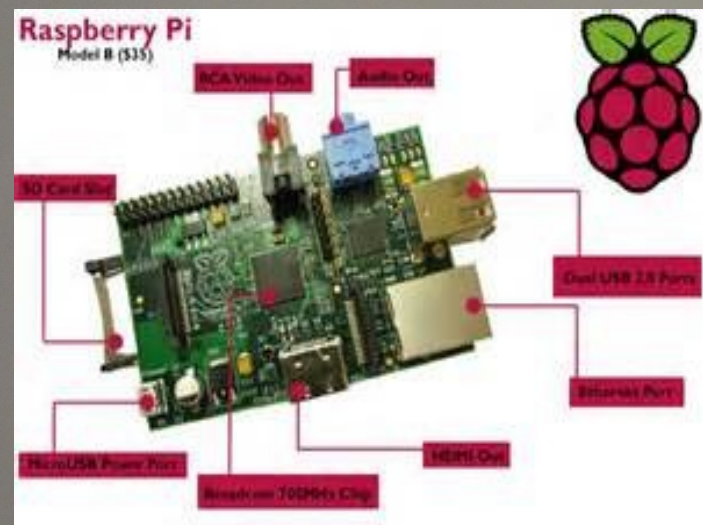
J.M.Pearce. Return on Investment for Open Source Hardware Development. *Science and Public Policy* 43(2),192-195 (2016).

Michigan Tech

Michigan Technological University
Open Sustainability Technology
Research Group



Case Study: Bespoke OS Syringe Pumps



Bas Wijnen, Emily J. Hunt,
Gerald C. Anzalone, Joshua
M. Pearce, 2014. Open-
source Syringe Pump Library,
PLoS ONE 9(9): e107216



of FOSH for Science

Syringe Pump: Savings \$153-\$2,442/pump (single, double)

Designs downloaded >1k times by Feb 2015

Downloaded Substitution Value \$168k-\$2.5m

Assume \$30k for development, 52% overhead

ROI of 750%-12,000%

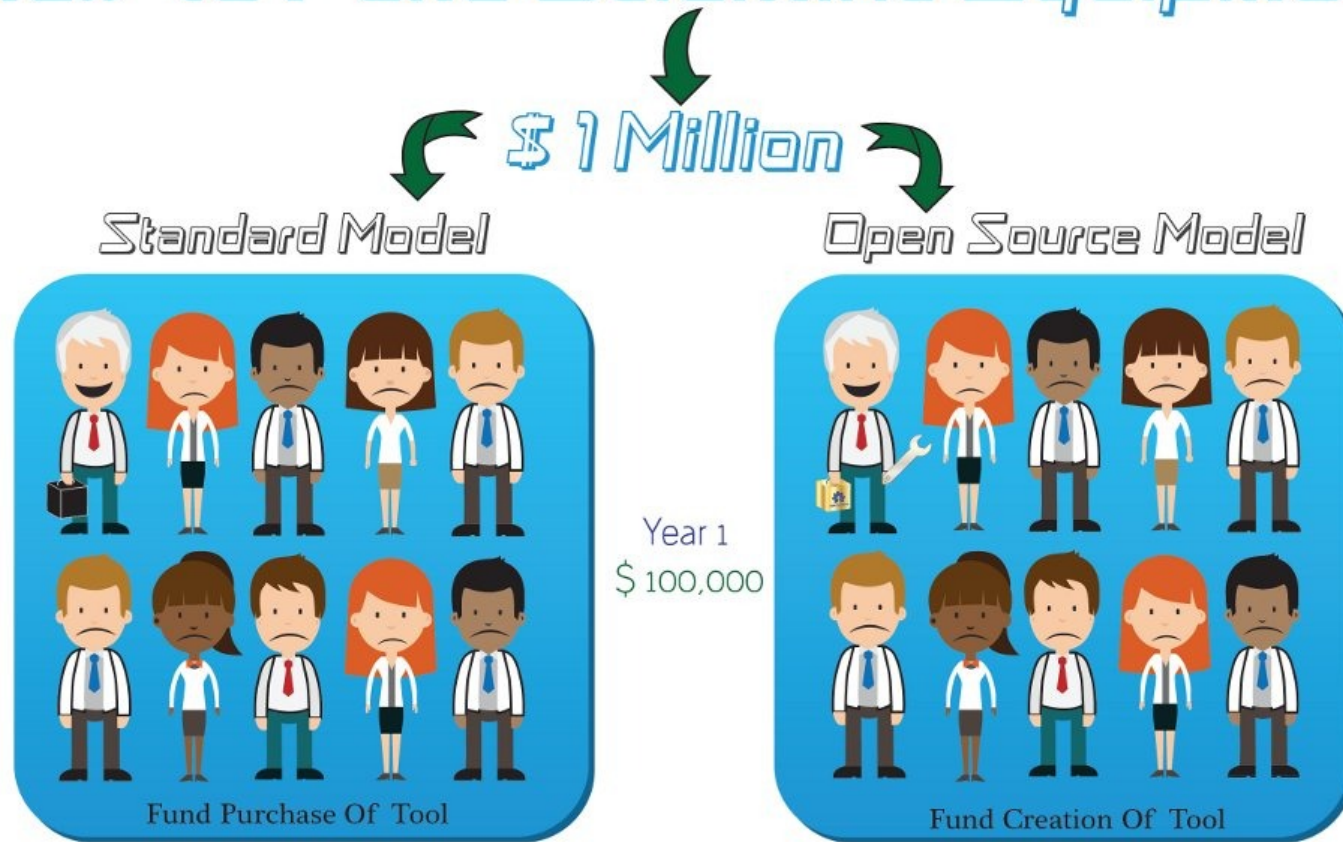


Michigan Tech

Michigan Technological University
Open Sustainability Technology
Research Group



How to Fund Scientific Equipment



* Only about 10% of NSF and NIH grants are funded

FASTER

	Black Box Proprietary Scientific Hardware No Control		Open Source Scientific Hardware Equivalent		Open Source Hardware Design		Open innovation results in better performance
---	---	---	---	---	-----------------------------	---	---

* Open source scientific hardware costs ~10% of proprietary hardware (Pearce, J.M. Open Source Lab, Elsevier, 2014).

Michigan Tech

Michigan Technological University
Open Sustainability Technology
Research Group



Proprietary



Year 2
\$ 100,000



Year 3 to 10
\$ 100,000
per year

FOSH



Michigan Tech

Michigan Technological University
Open Sustainability Technology
Research Group



Total

Proprietary



Only 10 scientists funded for 10 tools, most out of date.

90% of scientists remain unfunded.

Open Source Hardware (OSH)



91% of scientists funded, 91 state-of-the-art research tools, all open and easily upgrade-able for the cost of materials

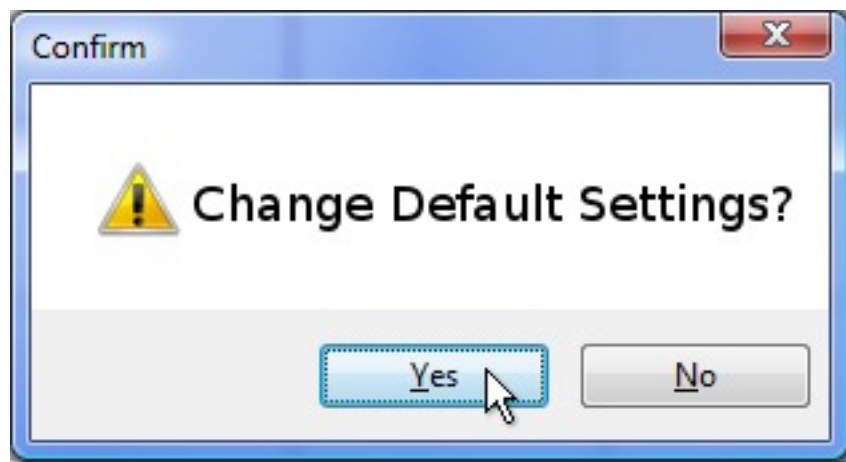
Michigan Tech

Michigan Technological University
Open Sustainability Technology
Research Group



Policy to Support FOSH and 3-D Printable Scientific Hardware

- 1) Task force - identify strategic goals, high ROI FOSH scientific tools,
- 2) Federal funding for scientific FOSH identified,
- 3) Free on-line catalog of validated scientific FOSH,
- 4) Purchasing policy preferences for FOSH for all government funded projects,
- 5) Supporting a maker space at all public universities, and
- 6) RepRap 3-D printer in every school.



Michigan Tech

Michigan Technological University
Open Sustainability Technology
Research Group



Where are we?

- 1) Task force - identify strategic goals, high ROI FOSH scientific tools,
- 2) Federal funding for scientific FOSH identified,
- 3) Free on-line catalog of validated scientific FOSH
- 4) Purchasing policy preferences for FOSH for all government funded projects,
- 5) Supporting a maker space at all public universities (no longer uncommon)
- 6) RepRap 3-D printer in every school
→ fastest growing segment of 3DP market (Wohlers).



Michigan Tech

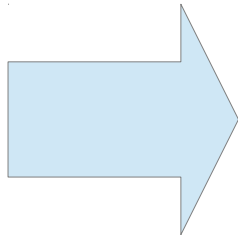
Michigan Technological University
Open Sustainability Technology
Research Group



Step 1.

Data – > Find already OS, and then low hanging fruit

Spectrophotometer - Shimadzu Model# UV-1800	LE	UV-1800	S	▶	8,713.00
Spectrophotometer - Shimadzu Model# UV-1800	LE	UV1800	CS	▶	8,713.00
000	▶LE	7200-000	720000541		8,819.37
Freezer, Revco Upright, Model ULT2586-10-A46	LE	ULT2586-10-A46	04	▶	11,442.54
Molecular Imager GS-800 Calibrated Densitometer	LE	GS-800	F09100005		13,460.80
Compact Sonde Water Quality Sensor, YSI 6920V	LE	6920U2	10B 101543		8,934.82
Compact Sonde Water Quality Sensor, YSI 6920V	LE	6920U2	10B 101541		8,934.82
Compact Sonde Water Quality Sensor, YSI 6920V	LE	6920U2	10B 101542		8,934.82
Compact Sonde Water Quality Sensor, YSI 6920V	LE	6920U2	10G100698		9,958.50
Rotor	▶LE	5305	5305ZK609840		6,706.00
Fume Hood, AirClean Systems 32" Ductless Enclosure	LE	AC730C, 700 Series	AC730C-926		5,159.00
Microscope, Inverted, Olympus Model CKX31	LE	CKX31SF	0F57967		8,908.85
StereoMicroscope, Olympus Model SZX16 (P0083779)	LE	SZX16	OJ65407		33,270.70
Shaker, Eppendorf Incubated Benchttop, Model I-24	LE	I Series 24	011051978		5,717.00
Ion Chromatography System, ICS-900, Dionex	LE	ICS-900			26,382.22
CO2 Incubator, Heracell 150i, Thermo Scientific, 120V	LE	Heracell 150i	41154823		5,005.00
Shaker, Eppendorf Incubated Benchttop, Model I-24	LE	I Series 24	010951433		6,405.00
X Unit	▶LE	X-AAF-1001X	▶510B0426		15,260.00



Michigan Tech

Michigan Technological University
Open Sustainability Technology
Research Group



The Future (not real), yet...

ARTICLES

PUBLISHED ONLINE: 18 MAY 2015 | DOI: 10.1038/NANO.2015.89

nature
nanotechnology

Black silicon solar cells with interdigitated back-contacts achieve 22.1% efficiency

Hele Savin^{1*}, Päivi Repo¹, Guillaume von Gastrow¹, Pablo Ortega², Eric Calle², Moises Garin² and Ramon Alcubilla²

The nanostructuring of silicon surfaces—known as black silicon—is a promising approach to eliminate front-surface reflection in photovoltaic devices without the need for a conventional antireflection coating. This might lead to both an increase in efficiency and a reduction in the manufacturing costs of solar cells. However, all previous attempts to integrate black silicon into solar cells have resulted in cell efficiencies well below 20% due to the increased charge carrier recombination at the nanostructured surface. Here, we show that a conformal alumina film can solve the issue of surface recombination in black silicon solar cells by providing excellent chemical and electrical passivation. We demonstrate that efficiencies above 22% can be reached, even in thick interdigitated back-contacted cells, where carrier transport is very sensitive to front surface passivation. This means that the surface recombination issue has truly been solved and black silicon solar cells have real potential for industrial production. Furthermore, we show that the use of black silicon can result in a 3% increase in daily energy production when compared with a reference cell with the same efficiency, due to its better angular acceptance.

Black silicon (b-Si)—as its name implies—absorbs light very efficiently for a wide range of wavelengths and, as a result, appears black to the naked eye. Its high absorption is based on gradual matching of the refractive index at the silicon/air interface using small nanostructures with dimensions below the wavelength of the incident light¹. Various shapes (including nanocones², nanowires³, microwires⁴ and porous silicon⁵) have been used to achieve excellent light management effects. Because of its many superior properties, b-Si has potential for a range of applications, such as self-cleaning surfaces⁶, microelectromechanical systems⁷, ion mobility spectrometers⁸, terahertz emitters⁹, drug analysis¹⁰, photodetectors¹¹ and antibacterial surfaces¹².

Black silicon would also appear to be an ideal material for photovoltaics due to its outstanding light management properties under the solar spectrum. In addition to boosting efficiency, b-Si can provide significant savings in manufacturing costs as there is no need to deposit a separate antireflection coating. The main challenges that have hindered the use of b-Si in photovoltaics are related to increased surface recombination due to the larger surface area of the nanostructures, and the situation is even more challenging in a conventional front-contacted solar cell structure due to Auger recombination at these highly doped nanostructures³. This means that a high number of light-generated electron-hole pairs are lost in the nanostructures instead of being collected at the contacts, reducing the efficiency. Auger recombination can be avoided by using an interdigitated back contact (IBC) solar cell design where the junction and the contacts are placed at the back of the cell¹³, but the recombination problem due to the larger surface area remains unsolved. To date, the surface passivation issue has generally been addressed by rather conventional methods, such as depositing silicon nitride by means of plasma-enhanced chemical vapour deposition¹⁴ or with thermally grown silicon dioxide¹⁵, resulting in tradeoffs between reflectance and recombination. The final efficiency has therefore been limited by recombination at the increased b-Si surface, and the reported

efficiencies have remained well below 20% (18.2% with a surface area of 0.8 cm²). However, our preliminary experiments on pin-hole-free and highly conformal atomic layer deposited (ALD) thin films combined with the chemical and field-effect passivation ability of Al₂O₃ (ref. 16) have shown promising results in overcoming the problematic surface recombination issue in b-Si¹⁷. Minority carrier lifetimes in the millisecond range indicate excellent surface passivation of b-Si and are in the range needed for high-efficiency solar cells (>20%)^{17,18}.

Previous b-Si solar cell results have been limited to those from conventional front-side aluminium back surface field (Al-BSF) structures or ultrathin back-contacted cells¹³, probably because these structures are less sensitive to front surface recombination. Here, we study the potential of ALD Al₂O₃ passivated b-Si to address the above-mentioned surface recombination problem present in nanostructured surfaces. We select a solar cell design that is known to be extremely sensitive to surface recombination—a thick interdigitated back-contact back-junction (IBC) solar cell¹³. In IBC cells, a majority of the photogenerated charge carriers have to diffuse a long distance from the front surface to the back side of the cells. A thick IBC cell is thus a very demanding structure even for conventionally textured solar cells. If b-Si works in this highly demanding structure, then the surface recombination challenge can be considered solved and b-Si should also be applicable to other cell structures.

Reflectance and surface recombination

Different methods for fabricating b-Si have been introduced, such as laser texturization¹⁹, plasma immersion ion implantation¹⁴ or metal-assisted wet etching²¹. Here, we use cryogenic deep reactive ion etching (DRIE) as it has multiple advantages: it is fast and inexpensive, there is no dependence on crystalline orientation, and there is no requirement for mask layers²². As can be seen in Fig. 1a, etching results in random nanoscale structures with a typical height of ~800 nm and width of 200 nm. A precise description of

¹Department of Micro and Nanosciences, Aalto University, Tietoie 3, Espoo 02150, Finland. ²Departament d'Enginyeria Electrònica, Universitat Politècnica de Catalunya, Jordi Girona 1-3, Mòdul C4, Barcelona 08034, Spain. *e-mail: hele.savin@aalto.fi

far from the equator, the increase is more important than when insolation is lower (winter) and this asymmetry grows with latitude. As can be seen in Fig. 5d, at 40° of latitude the increase is more than 2.5% during the four months with less insolation. Details of the calculation procedure are provided in the Methods.

Our results show that the b-Si is no longer limiting the cell efficiency, so further improvements should be possible by improving the cell structure. For example, even higher efficiencies could be expected by optimizing the emitter coverage. Other improvements could be implemented in current IBC structures to increase fill factor (FF) and V_{oc} values. For instance, a thicker aluminium layer in fingers and busbars would reduce ohmic losses, thereby achieving higher FF values. Moreover, an optimized phosphorus doping profile in the low and high doped emitter regions might further decrease the emitter saturation current density, J_{em} , increasing V_{oc} accordingly. Therefore, with realistic improved values of FF > 81% and V_{oc} > 675 mV, and assuming the excellent J_{sc} (42.2 mA cm⁻²) value achieved in this study, efficiencies well beyond 23% might be expected soon. Furthermore, because Al₂O₃ passivation has been reported to work on n-type surfaces as well²⁰, we plan to use the approach reported here for an n-type

p-type, b-Si IBC solar cell, with greater than 22% efficiency with a surface area of 9.0 cm². In the record cell we can use its optimal surface reflectance without affecting surface recombination, due to the outstanding surface passivation achieved with conformal ALD Al₂O₃. The use of a surface sensitive 280-µm-thick IBC structure proves that surface recombination, which has been hindering the use of b-Si in photovoltaics, is no longer a limiting factor. This should pave the way for even higher efficiencies in b-Si cells, not only in IBC structures but also in existing and new solar cell concepts.

Methods

Methods and any associated references are available in the online version of the paper.

Received 12 February 2015; accepted 25 March 2015; published online 18 May 2015

References

1. Clapham, J. & C. C. Reduction of lens reflection by the 'moth eye' principle. *Nature* **12**, 187 (1873).

NATURE NANOTECHNOLOGY | VOL 10 | JULY 2015 | www.nature.com/naturenanotechnology

627



ELSEVIER

HardwareX

open access



Open source 3-D printable atomic layer deposition system

Show more

<https://doi.org/10.1016/j.johx.2016.07.001>

Under a Creative Commons license

Bill of Materials
CAD and 3-D printable STLs
Electronics Schematics- Board design
Build Instructions
Firmware
Software
Recipes
Data

3DP + OSH = Ability to Immediately



Stand on the Shoulders of Giants

Michigan Tech

Michigan Technological University
Open Sustainability Technology
Research Group

